THE JOURNAL OF BIOLOGICAL CHEMISTRY VOL. 281, NO. 4, pp. 2071–2078, January 27, 2006

Stathmin Strongly Increases the Minus End Catastrophe Frequency and Induces Rapid Treadmilling of Bovine Brain Microtubules at Steady State *in Vitro*[*] [S]

Received for publication, September 29, 2005, and in revised form, November 11, 2005 Published, JBC Papers in Press, November 28, 2005, DOI 10.1074/jbc.M510661200

Tapas Manna[‡1], **Douglas Thrower**[‡1], **Herbert P. Miller**[‡], **Patrick Curmi**[§], **and Leslie Wilson**[‡2]

From the [‡]*Department of Molecular, Cellular, and Developmental Biology, University of California, Santa Barbara, California 93106 and* [§]*Laboratoire Structure et Reconnaissance des Biomolécules, EA3637, Université Evry-Val d'Essonne, rue du père Jarlan, 91025 Evry, France*

Stathmin is a ubiquitous microtubule destabilizing protein that is believed to play an important role linking cell signaling to the regulation of microtubule dynamics. Here we show that stathmin strongly destabilizes microtubule minus ends *in vitro* at steady state, conditions in which the soluble tubulin and microtubule levels remain constant. Stathmin increased the minus end catastrophe frequency ~13-fold at a stathmin:tubulin molar ratio of 1:5. Stathmin steady-state catastrophe-promoting activity was considerably stronger at the minus ends than at the plus ends. Consistent with its ability to destabilize minus ends, stathmin strongly increased the treadmilling rate of bovine brain microtubules. By immunofluorescence microscopy, we also found that stathmin binds to purified microtubules along their lengths *in vitro*. Co-sedimentation of purified microtubules polymerized in the presence of a 1:5 initial molar ratio of stathmin to tubulin yielded a binding stoichiometry of 1 mol of stathmin per ~14.7 mol of tubulin in the microtubules. The results firmly establish that stathmin can increase the steady-state catastrophe frequency by a direct action on microtubules, and furthermore, they indicate that an important regulatory action of stathmin in cells may be to destabilize microtubule minus ends.

Stathmin, also called Op18, is widely expressed in organisms ranging from *Drosophila* to humans and is especially highly expressed in the developing nervous system (1–4). Its expression is also elevated in a number of leukemias and solid tumors, which has led to the suggestion that it may be involved in tumorigenesis (5). The extensive phosphorylation of stathmin by various kinases activated during cell proliferation and differentiation (6, 7) together with its ability to destabilize microtubules and to increase the frequency by which microtubule plus ends switch from growth to rapid shortening (8, 9) has led to the idea that it plays an important role in linking cell signaling to the regulation of microtubule dynamics (7, 10–12).

The dynamic behaviors of microtubules play essential roles in their cellular functions (13, 14). In one form of dynamics, treadmilling, microtubules grow at their plus ends and shorten at their minus ends without changing lengths (15–18). It is hypothesized that the treadmilling rate is controlled by the tubulin dissociation rate constant at the minus ends (17). In the second form, dynamic instability, microtubule ends switch stochastically between periods of growth and shortening (19). With purified microtubules, dynamic instability occurs at both the plus and minus ends, with dynamic instability at plus ends more robust than at the minus ends (20, 21). In cells the minus ends of microtubules do not grow and, thus, do not undergo dynamic instability (22, 23). They are either capped and stable or they shorten persistently (22, 23).

The mechanisms responsible for controlling microtubule dynamics in cells are not well understood. A number of plus end destabilizing proteins have been identified including XKCM1/MCAK and stathmin (8, 24–27). These proteins have been called "catastrophe factors" because they can increase the frequency with which plus ends switch from growth to shortening (8, 9, 24–27). Only a few proteins have been identified that destabilize microtubules at their minus ends. Among these are the KinI kinesin KLP10A, which has been shown to depolymerize the minus ends of spindle microtubules in *Drosophila* (28), and XKCM1 and XKIF2, other members of the Kinesin 13 (Kin I) superfamily which have been shown to destabilize artificially stabilized minus ends *in vitro* (29). Minus ends of microtubules tethered at centrosomes are thought to be blocked and not dynamic (22, 23). However, the minus ends of non-attached microtubules can undergo shortening and sometimes can continuously depolymerize as their plus ends grow in a treadmilling fashion (30, 31). In addition, whereas the minus ends of spindle microtubules are tethered at the spindle poles, they are not blocked and continuously depolymerize. Coupled with growth at the plus ends of such microtubules, there is a pole-ward treadmilling-like flow of tubulin from the plus to minus ends (32, 33). The mechanisms responsible for controlling microtubule shortening at their minus ends are under intense study (28–33).

One possible regulator of minus end microtubule dynamics is the microtubule destabilizing protein, stathmin. Stathmin has been shown to increase the catastrophe frequency at the plus ends of purified microtubules (9), of microtubules in *Xenopus* cell extracts (8), and of microtubules in living cells (34–36). Evidence suggesting that stathmin might associate with the minus ends of microtubules was obtained in HeLa cells, where stathmin was shown by immunofluorescence microscopy to localize at the mitotic spindle poles (37).

The mechanisms by which stathmin destabilizes microtubules and increases the catastrophe frequency have been focus of much study. It is clear that sequestration of soluble tubulin by stathmin and the resulting reduction in the tubulin concentration can increase the catastrophe frequency (a switch from microtubule growth to shortening) and can also decrease the amount of microtubule polymer (9, 11, 38). Although direct evidence for the ability of stathmin to bind to microtubules has been lacking, it has been suggested that stathmin may increase the plus end catastrophe frequency by directly interacting with microtubules (9,

* This work was supported by United States Public Health Service Grant NS13560 (to L. W.) and a Genopole® Actualités de la Génomique et des Biotechnologies grant (to P. C.). The costs of publication of this article were defrayed in part by the payment of page charges. This article must therefore be hereby marked "*advertisement*" in accordance with 18 U.S.C. Section 1734 solely to indicate this fact.

[S] The on-line version of this article (available at http://www.jbc.org) contains supplemental material.

[1] These authors contributed equally to this work.

[2] To whom correspondence should be addressed. Tel.: 805-893-2819; Fax: 805-893-8094; E-mail: Wilson@lifesci.ucsb.edu.

11). Specifically, Howell *et al.* (9) found that under net microtubule assembly conditions (presteady state), stathmin increased the plus end catastrophe frequency without reducing the microtubule growth rate, indicating that stathmin might act directly on the microtubules themselves. However, analysis of microtubule dynamics under presteady-state conditions, when the free tubulin concentration is higher than what it would be at steady state and the polymer mass is increasing, would not reveal the complete effects of stathmin because changes in the soluble tubulin concentration and polymer level could mask some of its direct actions on the microtubules.

In the present work we analyzed the effects of stathmin on microtubule dynamic instability *in vitro* at both minus and plus ends at physiological pH, pH 7.2, and polymer mass steady state. At these conditions the soluble tubulin was maintained at the true steady-state critical concentration, and the microtubule level remained constant so that the direct actions of stathmin on the microtubules could be determined unambiguously. We found that stathmin strongly increases the steady-state catastrophe frequency at the minus ends and that its catastrophe-promoting activity is considerably stronger at minus ends than at plus ends. Consistent with its ability to destabilize microtubule minus ends, stathmin increased the treadmilling rate of microtubule-associated protein (MAP)[3]-rich microtubules *in vitro*. As predicted from its action on dynamic instability and treadmilling at steady state, we also found that stathmin binds to microtubules *in vitro*. The results support the idea that stathmin might regulate microtubule dynamics in cells by directly interacting with microtubules and further indicate that an important action of stathmin in cells might be to destabilize microtubule minus ends.

EXPERIMENTAL PROCEDURES

Tubulin and Stathmin—MAP-rich bovine brain microtubule protein (~ 20% MAPs and 80% tubulin) and tubulin derived from the microtubule protein were purified as described previously (21). The cloning and expression of human recombinant stathmin has also been previously described (39). The concentration of stathmin was determined by amino acid analysis.

Video Microscopy—Purified tubulin (17 μM) was assembled onto the ends of sea urchin (*Strongylocentrotus purpuratus*) axoneme seeds at 30 °C in the presence and absence of stathmin in 87 mM Pipes, 36 mM Mes, 1.4 mM $MgCl_2$, 1 mM EGTA, pH 7.2 (PMME buffer) containing 2 mM GTP (20, 21) and incubated at 30 °C for 40 min to achieve steady state. Attainment of true steady state of the seeded suspension was verified in the following way. Tubulin (17 μM) was added to a suspension of axoneme seeds at the same concentration used in the dynamic instability experiments, and the kinetics of microtubule assembly were determined both by light scattering at 350 nm and by sedimentation. The number concentration of axoneme seeds was ~50 axonemes/μl, which by video microscopy resulted in 5–8 axonemes per field of view (300 μm^2). There was a time-dependent increase in the microtubule polymer mass, with the plateau not reached until 35–40 min after initiation of assembly, after which the polymer level remained stable. We quantified the amount of soluble tubulin present once steady state had been achieved (40 min) after separating the pellet and supernatant by centrifugation and determined that the microtubule pellet contained 40% of the total tubulin. Thus, a large fraction of the initial soluble tubulin polymerized into microtubules in the seeded assembly system used for video analysis (data not shown). At steady state, the dynamics were significantly different from presteady-state conditions (supplemental data).

The stathmin concentrations used were 1.7 and 3.4 μM, respectively. Time-lapse images of microtubule plus and minus ends were obtained at 30 °C by video-enhanced differential interference contrast microscopy. Growth rates, shortening rates, and transition frequencies were determined as previously described (21). Ends were designated as plus or minus on the basis of the growth rates, the number of microtubules that grew at opposite ends of the seeds, and the relative lengths of the microtubules (20, 21). End designation was confirmed with *Chlamydomonas* flagella axonemes, which exhibit a bifurcation at their plus ends (40) (data not shown). We considered microtubules to be growing if they increased in length >0.3 μm at a rate >0.3 μm/min. Shortening events were identified by a >1-μm length change at a rate >2 μm/min. Microtubules that changed <0.3 μm/min over a duration of 4 data points were considered to be in an attenuated state. Between 30 and 90 microtubules were analyzed for each condition.

GTP Hydrolysis—Polymerization mixtures containing tubulin alone or a stathmin:tubulin molar ratio of 1: 5 were prepared exactly as in dynamic instability experiments. After 40 min of incubation at 30 °C, reactions were pulsed with [γ-^{32}P]GTP. Samples were collected at 10-min intervals for 1 h and subjected to thin layer chromatography to separate [γ-^{32}P]GTP from γ-^{32}Pi. The amount of remaining [γ-^{32}P]GTP was quantified by using a Bio-Rad Molceular Imager GS.

Determination of the Critical Tubulin Subunit Concentration—Solutions of tubulin free of MAPs at either pH 6.8 or 7.2 at concentrations ranging from 2 to 20 μM containing either no stathmin (controls) or 2 μM stathmin in PMME buffer with 1.5 mM GTP were polymerized to steady state for 40 min at 37 °C. Polymerization was induced with 10% Me_2SO. The microtubules were then sedimented by centrifugation at 150,000 × *g* at 35 °C for 1 h. Polymer pellets were re-suspended in ice-cold PMME buffer to depolymerize the microtubules. The amount of sedimented protein was determined and plotted against the initial tubulin concentration. The total soluble tubulin concentration for polymerization in the absence and presence of stathmin were determined from the *x* axis intercept of linear regression lines through each data set (41).

Stathmin Binding to Microtubules—We analyzed stathmin binding to microtubules by polymerizing purified tubulin (40 μM) with 4% glycerol seeds and stabilizing with 1 μM taxol. After 20 min, wild-type-stathmin (8 μM) or P16 stathmin was added to the preassembled microtubules, and incubation was continued for an additional 30 min. Microtubules were sedimented onto coverslips through 50% sucrose cushions containing 1 μM taxol. Coverslips were treated with a mixture of primary antibodies against α-tubulin (DM1A mouse monoclonal (1:500)) (Sigma) and stathmin (rabbit antiserum (1:200)) (Calbiochem) followed by the addition of secondary antibodies (donkey anti-mouse Cy3 and goat-anti-rabbit fluorescein). It was confirmed by Western blot analysis that the primary antibody against stathmin used in this experiment has similar affinity for both wild-type and P16 stathmin (not shown). Immunofluorescence images were obtained using Metamorph 4.6. For quantitation of stathmin binding to microtubules, tubulin (40 μM) and stathmin (8 μM) were assembled with 1% glycerol seeds in PMME buffer for 40 min at 37 °C. The microtubules were then sedimented through 30% sucrose cushions, and the pellets were resuspended and subjected to SDS-PAGE followed by Coomassie Blue staining. The amount of stathmin bound to the microtubules was determined by densitometric quantitative comparison with a known standard stathmin band by using EPI-CHMI darkroom scanner. The amount of protein in each pellet was determined before electrophoresis

[3] The abbreviations used are: MAP, microtubule-associated protein; PIPES, piperazine-1,4-bis(2-ethanesulfonic acid); Mes, 4-morpholineethanesulfonic acid.

by a Bradford protein assay (42), and the tubulin concentration was determined after subtraction of the quantity of bound stathmin. Control experiments with P16 stathmin (8 μM) were carried out in a similar manner.

Treadmilling Rates—The treadmilling rate was determined by measuring the incorporation of [^{3}H]GTP into MAP-rich microtubules at steady state using a glass fiber filter trapping assay (43). Microtubule protein (3 mg/ml) was polymerized to steady state for 30 min at 30 °C in 100 mM Pipes, 1 mM EGTA, and 1 mM $MgSO_4$, 0.02% sodium azide, pH 7.2 (PEM buffer) containing 0.1 mM GTP and a GTP regenerating system (10 mM acetyl phosphate and 1.5 unit/ml of acetate kinase). Incubations were carried out for an additional 25 min in the absence and presence of a 1:7 molar ratio of stathmin to tubulin. Then 600 μl of the polymerized microtubule suspension was mixed with 15 μl of [^{3}H]GTP (15 μCi). Portions of the suspension (40 μl each) were then removed over a 40-min time period and added to 4 ml of stabilizing buffer consisting of PEM containing 30% glycerol, 10% Me_2SO, and 5.6 mM ATP to stabilize the microtubules. The stabilized microtubules were collected by filtration onto GF/F glass fiber filters, which were then washed and counted in a scintillation counter ("Experimental Procedures"). Samples were prepared for electron microscopy 25 min after the addition of stathmin to determine the microtubule mean lengths and the microtubule polymer mass. Samples for electron microscopy of the control were taken at the same time.

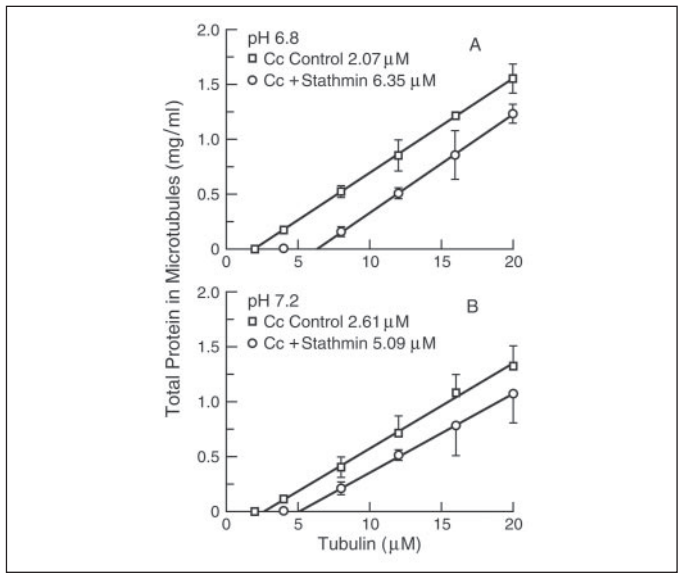

FIGURE 1. **The steady-state total soluble tubulin concentration "critical concentration" (C_c) in the absence and presence of 2 μM stathmin (see "Experimental Procedures").** Stathmin (2 μM) with increasing concentrations of tubulin ranging from 2 to 20 μM was polymerized to steady state at pH 6.8 (*A*) and pH 7.2 (*B*). *Squares*, controls (absence of stathmin); *circles*, presence of stathmin. C_c, critical concentration.

RESULTS

Stathmin Increases the Steady-state Catastrophe Frequency Strongly and Preferentially at the Minus Ends at Physiological pH—We wanted to analyze the effects of stathmin on dynamic instability at physiological pH. We chose pH 7.2 because a sampling of published intracellular pH values ranged from a low of 7.0 (44) to a high of 7.4 (45), and a comparison of reported pH values in 12 mammalian cell types yielded a mean pH of 7.20 ± 0.12 (44–54).

It has previously been shown that stathmin tubulin-sequestering activity decreases significantly as the pH is raised above pH 6.8 (38, 55). To determine whether this occurs upon increasing the pH from 6.8 to 7.2 and how it affects the soluble tubulin concentration in the microtubule suspension, we assembled different concentrations of tubulin to polymer mass steady state in the absence and presence of 2 μM stathmin and determined the soluble tubulin concentration below which no microtubules could be detected (the tubulin subunit critical concentration, C_c). At pH 6.8 in the absence of stathmin, the soluble tubulin critical concentration was 2.07 μM. It has been shown that one molecule of stathmin can form a stable complex with two tubulin dimers *in vitro*, called a "T_2S complex" (38, 56, 57). If stathmin can sequester tubulin efficiently under these conditions, the total soluble tubulin concentration should increase to 6 μM because 2 μM added stathmin would sequester 4 μM tubulin, preventing it from assembling into microtubules. As shown Fig. 1, at pH 6.8 the total soluble tubulin concentration did indeed increase by ~4 μM (from 2.07 to 6 μM). Stathmin sequestered tubulin to a lesser degree at pH 7.2 than at pH 6.8. The total soluble tubulin concentration in the presence of 2 μM stathmin at pH 7.2 was increased by only ~ 2.5 μM, from 2.61 to 5.09 μM (Fig. 1*B*), indicating that stathmin sequesters tubulin ~40% less efficiently at pH 7.2 than at pH 6.8. These results indicate that an appreciable amount of free stathmin is present at steady state at pH 7.2, which could interact directly with microtubules (see Figs. 4 and 5). The data also indicate that little free stathmin must be available at pH 6.8.

We also wanted to analyze the effects of stathmin on microtubule dynamics at steady state, conditions in which the microtubule polymer mass and tubulin concentration remain constant, and a direct interaction of stathmin with microtubules can be determined unambiguously. This was accomplished by assembling tubulin into microtubules for 40 min before analysis to ensure attainment of steady state (see "Experimental Procedures"). The attainment of steady state in the absence and presence of the various stathmin concentrations used was verified by light scattering at 350 nm and sedimentation and occurred 35–40 min after initiation of polymerization (not shown). As shown in Supplemental Table 1, the dynamics of microtubules at steady state are significantly different from presteady-state conditions. As expected, the polymer mass was reduced by stathmin. Specifically, at the highest stathmin concentration used (3.4 μM, a 1:5 molar ratio of stathmin to tubulin), the polymer mass was reduced by only 20% as compared with the control (Supplemental Fig. 1). A tubulin concentration of 17 μM was chosen for these assays because it yielded measurable microtubule lengths under the conditions employed in this study, and the relatively low stathmin concentrations used ensured that the polymer levels were adequate to obtain measurable microtubule lengths.

The dynamic instability parameters at both plus and minus ends of steady-state microtubules are shown in Table 1, and the effects of stathmin on the catastrophe frequencies are shown in Fig. 2. At a stathmin: tubulin ratio of 1:10 and with the concentration of tubulin and stathmin 17 and 1.7 μM, respectively, stathmin increased the catastrophe frequency 2-fold at the plus ends. Surprisingly, it increased the catastrophe frequency 9-fold at the minus ends. At a stathmin:tubulin ratio of 1:5, the highest concentration that allowed measurable microtubule lengths, the catastrophe frequency increased almost 13-fold at the minus ends and only ~3-fold at the plus ends (Table 1, Fig. 2). The growth rate was not reduced, but rather, it increased slightly at both ends, and the percentage of time the microtubules spent growing also increased (Table 1). Stathmin did not significantly affect the shortening rate at either end, but it strongly increased the fraction of time that the microtubules shortened. It also decreased the fraction of time the microtubules remained in an attenuated state neither growing nor shortening detectably, and it increased the overall dynamicity of minus ends 6.7-fold and plus ends ~2-fold. Thus, at steady state and physio-

TABLE 1

Effects of stathmin on steady-state microtubule dynamic instability at pH 7.2

Tubulin concentration was 17 μM. Stathmin concentrations were 1.7 (1:10) and 3.4 μM (1:5). Data are given as the mean ± S.D. *n*, number of events.

	Stathmin:Tubulin ratio					
	0 (Control)	*n*	1:10	*n*	1:5	*n*
Plus end						
Growth rate μm min^{-1}	1.26 ± 0.53	55	1.51 ± 0.73	78	1.59 ± 0.67	104
Shortening rate μm min^{-1}	30.6 ± 18.2	33	30.6 ± 12.3	45	24.1 ± 15.2	77
Percent time growing	42.4		62.0		65.5	
Percent time shortening	2.8		5.9		6.6	
Percent time attenuated	54.7		32.1		27.8	
Catastrophe frequency min^{-1}	0.15 ± 0.03	32	0.31 ± 0.05	44	0.41 ± 0.05	77
Rescue frequency min^{-1}	1.74 ± 0.52	11	1.23 ± 0.37	30	1.14 ± 0.29	15
Dynamicity μm min^{-1}	1.24	87	2.15	123	2.19	181
Minus end						
Growing rate μm min^{-1}	0.90 ± 0.38	17	0.88 ± 0.45	61	1.06 ± 0.57	62
Shortening rate μm min^{-1}	30.7 ± 23.6	11	32.9 ± 23.1	23	25.3 ± 3.7	32
Percent time growing	6.0		31.9		33.0	
Percent time shortening	0.2		1.3		1.6	
Percent time attenuated	93.8		66.8		65.4	
Catastrophe frequency min^{-1}	0.01 ± 0.004	11	0.09 ± 0.02	22	0.13 ± 0.02	30
Rescue frequency min^{-1}	3.93 ± 1.49	7	4.23 ± 1.17	13	3.78 ± 1.01	14
Dynamicity μm min^{-1}	0.10	28	0.55	84	0.67	94

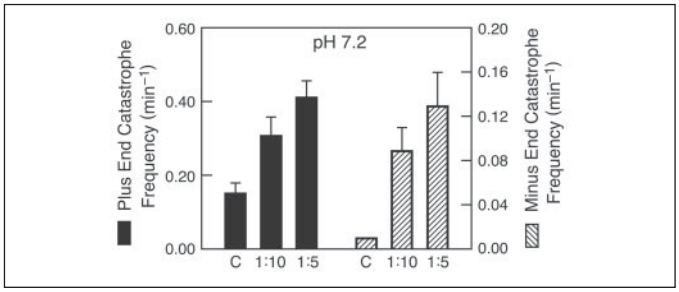

FIGURE 2. **Catastrophe frequencies in the absence and presence of stathmin at microtubule plus and minus ends at pH 7.2.** Molar ratios shown are of stathmin to tubulin. 17 μM tubulin was polymerized in the presence and absence of 1.7 and 3.4 μM stathmin to steady-state polymer mass at 30 °C before analysis of the microtubule dynamics (see "Experimental Procedures"). *C*, control.

logical pH *in vitro*, the most potent effects of stathmin on dynamic instability were to increase minus end catastrophe frequency and dynamicity.

Because stathmin can stimulate the GTPase activity of tubulin (55), we wanted to ensure that stathmin did not deplete the GTP required for maintaining steady state. We determined that stathmin did not detectably deplete the GTP at the highest ratio of stathmin to tubulin used (1:5) ("Experimental Procedures"; results not shown).

Stathmin Strongly Increases the Treadmilling Rate of MAP-rich Microtubules in Vitro—The robust increase in the minus end catastrophe frequency produced by stathmin suggested to us that it might increase the treadmilling rate. We previously obtained evidence indicating that the microtubule treadmilling rate is related to the differences in the critical subunit concentrations at opposite microtubule ends and have suggested that the rate might be largely controlled by the dissociation rate constant at the minus ends (17). For example, we modeled how small increases in the critical tubulin subunit concentration at minus ends could result in large increases in the treadmilling rate (17). To determine the effect of stathmin on treadmilling, experiments were performed with MAP-rich microtubules, which are intrinsically stable because of their high MAP content and display minimal dynamic instability (58). Treadmilling rates were determined by measurement of [^{3}H]GTP incorporation into the microtubules (43). This is a highly sensitive procedure that allows one to quantify the rate of GTP-tubulin incorporation at the microtubule ends at a molecular level (59) and, thus, allows accurate measurements of the microtubule treadmilling rate. This strategy is more sensitive than microscopy-based methods, which do not afford molecular resolution and do not require that the microtubules be tethered to surfaces, which could impair treadmilling (see "Discussion").

Microtubule protein was polymerized in the presence and absence of stathmin to steady state, after which the microtubules were pulsed with [^{3}H]GTP. The kinetics of [^{3}H]GDP-tubulin incorporation into the microtubules were determined, and the treadmilling rates were calculated from linear regression of the data ("Experimental Procedures"). As shown in Fig. 3, the rate of [^{3}H]GDP-tubulin incorporation into the microtubules was much more rapid in the presence of stathmin than in its absence. The treadmilling rate of the control microtubules calculated after determination of the mean microtubule lengths by electron microscopy was 1.32 μm/h/microtubule, and ~3% of the microtubules had become labeled in 40 min. A 1:7 molar ratio of stathmin to tubulin increased the treadmilling rate ~8-fold to 10.9 μm/h/microtubule, and in the presence of stathmin, ~34% of the microtubules were labeled. Similar rates were obtained in an identical replicate experiment (0.95 μm/h for control microtubules, 10.2 μm/ h in the presence of stathmin). To eliminate the possibility that stathmin might remove MAPs from the microtubules, which would also increase the treadmilling rate (17), the MAP content of the microtubules at different times during the analysis was quantified by SDS-PAGE and found to be unaffected quantitatively or qualitatively by the addition of stathmin (data not shown). No dynamic instability was detected by video microscopy with MAP-rich microtubules either in the presence or absence of stathmin at either microtubule end. Although stathmin did not detectably increase the dynamic instability of MAP-rich microtubules by video microscopy, it is to be expected that minus end shortening due to treadmilling (0.2 μm/min) could not have been detected by video microscopy. The data also demonstrate that rapid treadmilling occurs in the absence of significant dynamic instability (see "Discussion").

Stathmin Binds to Microtubules along Their Lengths in Vitro—The ability of stathmin to increase the steady-state catastrophe frequency and the treadmilling rate indicates that it must act directly on microtubules. Using two different approaches, we found that stathmin indeed binds to microtubules. In the first, microtubules were assembled to steady state at a 1: 5 molar ratio of stathmin to tubulin, and the amount of stathmin bound to the microtubules was determined by SDS-PAGE followed by densitometric analysis after sedimentation through sucrose cushions to ensure removal of any nonspecifically bound stathmin

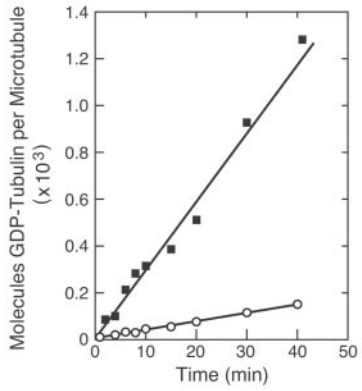

FIGURE 3. **Treadmilling incorporation of tubulin-GDP into steady-state microtubules assembled from MAP-rich microtubule protein in the presence (*squares*) and absence (*circles*) of stathmin.** The molar ratio of stathmin to tubulin was 1:7. The mean lengths of the control and the stathmin-treated microtubules were 22.2 μm and 20.3 μm, respectively.

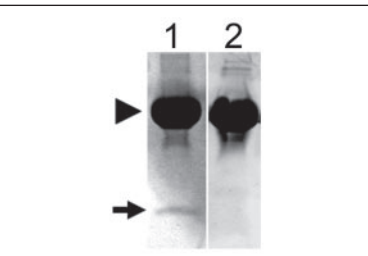

FIGURE 4. **Stathmin binding to microtubules *in vitro*.** Shown are Coomassie Blue-stained SDS-PAGE samples of microtubules (40 μM tubulin) assembled in the presence of 8 μM stathmin (*lane 1*) and in the presence of 8 μM P16 stathmin (*lane 2*) at pH 7.2 and sedimented through a 30% sucrose cushion ("Experimental Procedures"). The position of the 18-kDa stathmin band is indicated with an *arrow* and of the tubulin band with an *arrowhead*. The molar ratio of stathmin to tubulin in the microtubule pellets was 1:14.7 $\pm$ 1.8 (S.E., based on the results of three independent experiments).

("Experimental Procedures") (Fig. 4, *lane 1*). This experiment was repeated three times. Quantitation of the stathmin present in microtubule pellets revealed that 1 mol of stathmin was bound per 14.7 $\pm$ 1.8 mol of tubulin dimer in the microtubules. To further eliminate the possibility that the stathmin bound to the microtubules nonspecifically, we determined that P16 stathmin, a full-length stathmin phosphorylated at serine 16, which does not appreciably bind to tubulin (55, 60)[4], did not associate with the microtubules (Fig. 4, *lane 2*). Measurement of pixel intensities at the location on the gel where stathmin normally migrates did not reveal any values above background (Fig. 4, *lane 2*).

We also used antibodies to tubulin and stathmin to visually detect stathmin binding to the microtubules. Tubulin was first polymerized into microtubules and stabilized with 1 μM taxol before adding stathmin (1:5 ratio of stathmin to tubulin). The microtubules were then sedimented through sucrose cushions onto glass cover slips ("Experimental Procedures") and immunostained with antibodies specific to tubulin and stathmin. We found that stathmin was bound along the lengths of the microtubules (Fig. 5, *A* and *B*). Control experiments in which the microtubules were polymerized in the absence of stathmin did not exhibit any stathmin staining (Fig. 5, *C* and *D*). In the absence of the tubulin antibody, stathmin immunostaining appeared in the form of linear filaments identical to those observed when both tubulin and stathmin antibodies were present (data not shown). This experiment

[4] T. Manna, D. Thrower, M. O. Steinmetz, P. Curmi, and L. Wilson, unpublished data.

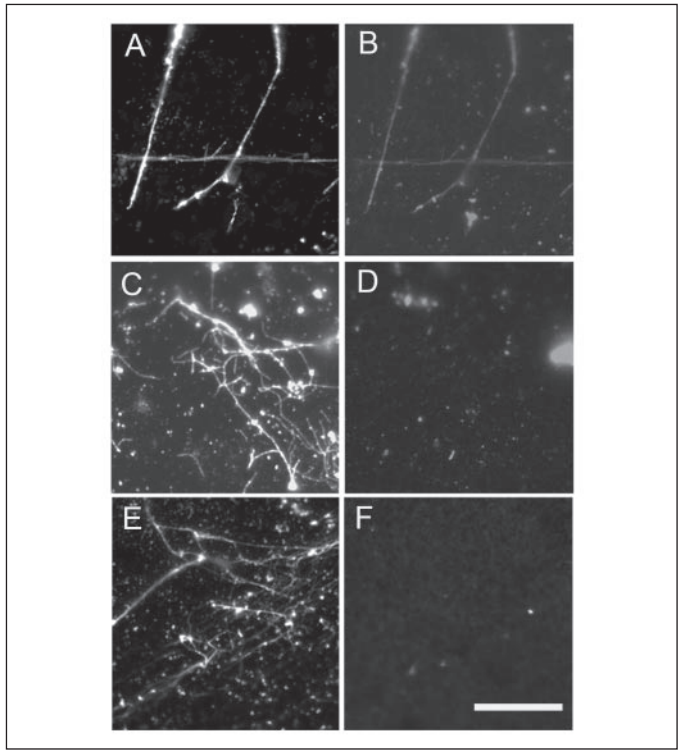

FIGURE 5. **Immunofluorescence images demonstrating stathmin binding along the lengths of microtubules *in vitro* ("Experimental Procedures").** Microtubules were assembled with 40 μM tubulin and 1 μM taxol before the addition of 8 μM stathmin or 8 μM P16 stathmin. Microtubules were co-immunostained with antibodies to α-tubulin (*A*, *C*, and *E*) or stathmin (*B*, *D*, and *F*). *Panels C*, *D*, and *E* show images of taxol-assembled microtubules to which no stathmin was added. We confirmed by Western blot analysis that the stathmin antibody had the same affinity for unphosphorylated and P16 stathmin. Images show typical results of at least three independent experiments. *Scale bar*, 5 μm.

also demonstrates that stathmin can bind directly to preformed microtubules. As a further control for possible nonspecific binding of stathmin to the microtubules, we also determined using the same procedure that P16 stathmin did not bind to the microtubules (Fig. 5, *E* and *F*).

DISCUSSION

By analyzing the effects of stathmin on microtubule dynamic instability at polymer mass steady state *in vitro*, a condition in which the total soluble tubulin concentration remains at the steady-state critical concentration (C_c) and does not change, we found that stathmin increases the catastrophe frequency at both minus and plus ends by a direct action on microtubules. By assembling microtubules to steady state onto axoneme seeds under identical conditions to those used in the video microscopy experiments, we determined that the microtubules analyzed by microscopy were at true steady state. We also confirmed that the dynamics parameters of microtubules at steady state were significantly different from presteady-state conditions (supplemental data).

The destabilizing effects of stathmin at the minus ends were considerably stronger than its effects at plus ends. At pH 7.2, a pH similar to that within mammalian cells, a ratio of stathmin to tubulin of 1:5 increased the catastrophe frequency ~13-fold at minus ends and only 3-fold at plus ends (Fig. 2). Such a strong effect at minus ends implies that stathmin may regulate microtubule disassembly dynamics at their minus ends in cells. For both ends, the increase in the catastrophe frequency in the absence of detectable slowing of the growth rate and no significant increase in the shortening rate strongly supports the hypothesis that the stathmin effect on the catastrophe frequency at steady state occurs by a direct interaction with the microtubules (Table 1). In direct

support of this idea, we determined that when stathmin was added to microtubules at a 1:5 molar ratio of stathmin to tubulin, one molecule of stathmin became bound per ~15 molecules of tubulin in the microtubules (Fig. 4). Using antibodies specific to stathmin, we further demonstrated that stathmin can bind directly to the microtubules along their lengths (Fig. 5). Related to its ability to destabilize minus ends, we also found that stathmin significantly increased the rate of microtubule treadmilling (Fig. 3).

Possible Action of Stathmin Directly on Microtubules —Evidence in support of the possibility that stathmin might bind to microtubules was initially obtained by Gavet *et al.* (61), who found that stathmin localized to mitotic spindles in HeLa cells. In addition, stathmin was shown to change the structure of microtubule ends in *Xenopus* crude extracts, an effect also indicating a direct interaction of stathmin with microtubules (62). However, stathmin does not appear to associate with microtubules to an extent detectable by immunofluorescence microscopy in interphase cells. It is reasonable to think that a large fraction of the stathmin in interphase cells might not be available to bind microtubules because most of it would be sequestered by soluble tubulin. However, a small fraction of free stathmin could still be available to interact with microtubules. Small quantities of microtubule-bound stathmin could create large effects on dynamics in the absence of appreciable changes in the soluble tubulin level. Such a mechanism is similar to how microtubule-targeted drugs such as taxol and vinblastine act. Substoichiometric quantities of drug molecules bound to microtubules produce powerful effects on dynamics in the absence of changes in polymer mass both *in vitro* and in living cells (for review, see Ref. 63).

In the present work we found that when stathmin and tubulin (1:5 molar ratio of stathmin to tubulin) were co-polymerized into microtubules and sedimented through sucrose cushions to remove any nonspecifically bound stathmin, stathmin co-sedimented with the microtubules (Fig. 4). To further eliminate the possibility that stathmin was binding nonspecifically to the microtubules, we determined that P16 stathmin, a stathmin construct phosphorylated at serine 16, did not bind to the microtubules (Fig. 4). Although the amount of bound stathmin protein was low, as evidenced by the staining intensities of the stathmin and tubulin bands, the molecular weight of stathmin is ~6-fold lower than tubulin dimers. On a molar basis, even if stathmin could fully saturate the microtubule by the binding of one molecule of stathmin to every two tubulin dimers in the microtubule, the amount of protein in the stathmin band could be no more than one-twelfth of the protein in the tubulin band. The bound stathmin was well below a saturating level and on a molar basis, yielded a stathmin:tubulin dimer ratio of 1:14.7 (±1.8). Using an *in vitro* immunofluorescence based microscopic assay and a similar stathmin to tubulin ratio of 1:5, we also visualized stathmin bound along the lengths of the microtubules (Fig. 5).

We can imagine three ways in which stathmin might bind to microtubules. One possibility is that free stathmin can bind to the exposed α tubulin subunits at the minus ends in a manner similar to how it binds to α_1 tubulin in the tubulin-stathmin (T_2S) complex (57). The stathmin N terminus might even facilitate the binding of free stathmin molecules to minus ends. Free stathmin could also bind to microtubule plus ends. Plus ends with their exposed β-tubulin subunits could permit the binding of stathmin in a similar fashion to how it binds to the β_2-tubulin subunit in the T_2S complex (57). For this, the stathmin N terminus must move out of the way, which could readily occur because this part of the protein is thought to be relatively unstructured in the absence of tubulin binding (56, 57). Finally, in similar fashion, free stathmin could bind along the lengths of the microtubules. Our immunofluorescence microscopy experiments demonstrating that stathmin can bind to preformed microtubules along their lengths strongly support this possibility (Fig. 5).

How could stathmin bound along the lengths of microtubules affect the gain and loss of tubulin subunits at microtubule ends? It has been shown previously that the T_2S complex organizes as a helix building block with a radius of curvature similar to that of the frayed protofilaments at the ends of depolymerizing microtubules (56, 57, 64). Increased numbers of such frayed protofilaments were indeed observed at the ends of microtubules in *Xenopus* extracts induced to depolymerize with stathmin (62). Although we suspect that the binding of stathmin to tubulin in the microtubule lattice in regions distant from the ends is not likely to produce such a curvature, microtubule-bound stathmin near or at microtubule ends might have such effects and could, thus, induce a transition to rapid shortening. Additional evidence indicating that the stathmin steady-state catastrophe-promoting activity is caused by the binding of free stathmin to the microtubules is derived from analysis of stathmin effects on steady-state dynamic instability at plus and minus ends at pH 6.8. We and others (38, 55) have found that stathmin binds to soluble tubulin very strongly at pH 6.8 (Fig. 1). At pH 6.8, where little free stathmin was available to bind to microtubules, stathmin did not increase the steady-state catastrophe frequency at minus ends and did so only weakly at the plus ends (data not shown).

Our data indicate that stathmin increased the catastrophe frequency much more strongly at minus ends than at plus ends. Because stathmin binds along the lengths of microtubules, one might expect that stathmin would increase the catastrophe frequency equally at the two ends. However, there is good precedent for such differential activity at the plus and minus ends with taxol, which like stathmin binds along the length of the microtubule. Taxol strongly suppresses dynamic instability at plus ends but not at the minus ends (65). The differences in stathmin ability to increase the catastrophe frequency at the plus and minus ends could be due differences in the way it binds to the plus and minus ends. If stathmin binds to the microtubule ends in a similar fashion as it binds to soluble tubulin dimers (57), the conformation of bound stathmin at the two ends would be different.

How might Stathmin Increase the Treadmilling Rate?—Microtubule treadmilling, like the treadmilling of actin filaments, has been hypothesized to be driven by the differences in the critical concentrations for tubulin addition at the opposite microtubule ends (17). However, Grego *et al.* (66) analyzed the dynamics of individual microtubules tethered to glass by fluorescent speckle microscopy and concluded that intrinsic treadmilling did not occur but, rather, arose from unbalanced dynamic instability at opposite microtubule ends. However, we would expect tethering of microtubules to glass along their lengths to impair treadmilling. In our previous work (17), MAP-free microtubules analyzed in the presence of 2% glycerol treadmilled rapidly (0.2 μm/min) in the absence of appreciable dynamic instability behavior, strongly supporting the idea that treadmilling is an intrinsic microtubule behavior that occurs independent of dynamic instability. In addition, rapid microtubule treadmilling occurs in living cells in the absence of length changes (16).

In this work we used microtubules that were strongly stabilized by brain MAPs and which did not display detectable dynamic instability behavior either in the absence or presence of stathmin. Stathmin strongly increased the incorporation of radiolabeled GTP-tubulin into the microtubules, and because it did so in the absence of dynamic instability, the incorporation must have been due to treadmilling. During a 40-min time span, steady-state control microtubules became radiolabeled at ~3% of their lengths, and thus, their treadmilling rate was 1.32 μm/h. At a 1:7 ratio of stathmin:tubulin, microtubules became labeled

at 34% that of their lengths, and thus, the treadmilling rate was increased ~8-fold (Fig. 3). In view of the strong ability of stathmin to increase the minus end catastrophe frequency, we suggest that stathmin increased the treadmilling rate by destabilizing the minus ends of the microtubules.

Possible Significance of the Catastrophe-promoting Activity of Stathmin at Microtubule Minus Ends and Regulation of Treadmilling in Cells—Dynamic instability does not appear to occur at microtubule minus ends in cells, and evidence thus far indicates that the minus ends do not grow but either remain in a paused state or persistently shorten (22, 23). Because stathmin can readily convert a growing or attenuated minus end to one that is shortening, the main function of stathmin in cells at the minus ends might be to destabilize these ends. Spindle microtubules in vertebrate cells continuously depolymerize at their minus ends in a treadmilling-like fashion by a process called pole-ward flux (32, 33), and it has been suggested that factors facilitating minus end depolymerization may play a role in pole-ward flux (33, 68, 69). Immunodepletion of the Kin1 kinesin KLP10A, which is localized to anaphase spindle poles in *Drosophila* S2 cells, has been shown to almost completely eliminate pole-ward flux (28). Although it has not been firmly established that KLP10A or homologs of KLP10A in other organisms are responsible for the generation of spindle flux, the results clearly show that KLP10A must play an important role in *Drosophila*. Because stathmin is localized at the spindle poles in mitotic HeLa cells (37), it is quite possible that it might play a role in increasing the rate of pole-ward tubulin subunit flow by destabilizing the minus ends. Although the catastrophe-promoting activity of stathmin is significantly attenuated by phosphorylation (60),[4] measurements of stathmin phosphorylation during mitosis have revealed that a fraction of the stathmin remains unphosphorylated even in cells blocked for extended periods in mitosis (61). Thus, some stathmin could remain active and might potentially contribute to tubulin flux in spindles.

A significant fraction of cytoplasmic microtubules in mammalian cells is not attached to centrosomes (30). Because stathmin is found throughout the cytoplasm (61), it could also increase the minus end disassembly of unattached microtubules (70). Disassembly at the minus ends of unattached microtubules has been recognized to contribute significantly to microtubule turnover in cells through the minus end pathway, especially in the regions near the cell center (22, 30, 70–73). Another interesting possibility is that the shortening rate at the minus ends of axonal microtubules or those in growth cones, which are not tethered at centrosomes, might be increased by stathmin, and thus, one of the functions of stathmin in axons might be to facilitate microtubule treadmilling or plus end growth (67, 74).

Acknowledgments—We thank Andre Sobel and Sylvie Lachkar for providing reagents and for helpful discussions and Michel Steinmetz for providing P16 stathmin. We also thank Mary Ann Jordan for critically reading the manuscript.

REFERENCES

1. Doye, V., Soubrier, F., Bauw, G., Boutterin, M. C., Beretta, L., Koppel, J., Vandekerckhove, J. & Sobel, A. (1989) *J. Biol. Chem.* **264,** 12134–12137
2. Amat, J. A., Fields, K. L. & Schubart, U. K. (1991) *Dev. Brain Res.* **60,** 205–218
3. Bieche, I., Maucuer, A., Laurendeau, I., Lachkar, S., Spano, A.J., Frankfurter, A., Levy, P., Manceau, V., Sobel, A., Vidaud, M. & Curmi, P. A. (2003) *Genomics* **81,** 400–410
4. Ozon, S., Guichet, A., Gavet, O., Roth, S. & Sobel, A. (2002) *Mol. Biol. Cell* **13,** 698–710
5. Roos, G., Brattsand, G., Landberg, G., Marklund, U. & Gullberg, M. (1993) *Leukemia* **7,** 1538–1546
6. Schubart, U. K., Xu, J., Fan, W., Cheng, G., Goldstein, H., Alpini, G., Shafritz, D. A., Amat, J. A., Farooq, M. & Norton, W. T. (1992) *Differentiation* **51,** 21–32
7. Sobel, A. (1991) *Trends Biochem. Sci.* **16,** 301–305
8. Belmont, L. D. & Mitchison, T. J. (1996) *Cell* **84,** 623–631
9. Howell, B., Larsson, N., Gullberg, M. & Cassimeris, L. (1999) *Mol. Biol. Cell* **10,** 105–118
10. Wittmann, T. & Waterman-Storer, C. M. (2001) *J. Cell Sci.* **114,** 3795–3803
11. Cassimeris, L. (2002) *Curr. Opin. Cell Biol.* **14,** 18–24
12. Wittmann, T., Bokoch, G. M. & Waterman-Storer, C. M. (2004) *J. Biol. Chem.* **279,** 6196–6203
13. Mitchison, T. J. (1988) *Annu. Rev. Cell Biol.* **4,** 527–549
14. Gelfand, V. I. & Bershadsky, A. D. (1991) *Annu. Rev. Cell Biol.* **7,** 93–116
15. Margolis, R. L. & Wilson, L. (1978) *Nature* **293,** 705–711
16. Rodionov, V. I. & Borisy, G. G. (1997) *Science* **275,** 215–218
17. Panda, D., Miller, H. P. & Wilson, L. (1999) *Proc. Natl. Acad. Sci. U. S. A.* **96,** 12459–12464
18. Chen, W. & Zhang, D. (2004) *Nat. Cell Biol.* **6,** 227–231
19. Mitchison, T. J. & Kirschner, M. W. (1984) *Nature* **312,** 237–242
20. Walker, R. A., O'Brien, E. T., Pryer, N. K., Soboeiro, M. F., Voter, W. A., Erickson, H. P. & Salmon, E. D. (1988) *J. Cell Biol.* **107,** 1437–1448
21. Panda, D., Jordan, M. A., Chu, K. C. & Wilson, L. (1996) *J. Biol. Chem.* **271,** 29807–29812
22. Rodionov, V. I., Nadezhdina, E. S. & Borisy, G. G. (1999) *Proc. Natl. Acad. Sci. U. S. A.* **96,** 115–120
23. Dammermann, A., Desai, A. & Oegema, K. (2003) *Curr. Biol.* **13,** 614–624
24. Wordeman, L. & Mitchison, T. J. (1995) *J. Cell Biol.* **128,** 95–104
25. Hunter, A. W., Caplow, M., Coy, D. L., Hancock, W. O., Diez, S., Wordeman, L. & Howard, J. (2003) *Mol. Cell* **11,** 445–457
26. Newton, C. N., Wagenbach, M., Ovechkina, Y., Wordeman, L. & Wilson, L. (2004) *FEBS Lett.* **572,** 80–84
27. Walczak, C. E., Mitchison, T. J. & Desai, A. (1996) *Cell* **84,** 37–47
28. Rogers, G. C., Rogers, S. L., Schwimmer, T. A., Ems-McClung, S. C., walczak, C. E., Vale, R. D., Scholey, J. M., & Sharp, D. J. (2004) *Nature* **427,** 364–370
29. Popov, A. V., Severin, F. & Karsenti, E. (2002) *Curr. Biol.* **12,** 1326–1330
30. Keating, T. J., Peloquin, J. G., Rodionov, V. I., Momcilovic, D. & Borisy, G. G. (1997) *Proc. Natl. Acad. Sci. U. S. A.* **94,** 5078–5083
31. Shaw, S. L., Kamyar, R. & Ehrhardt, D. W. (2003) *Science* **300,** 1715–1718
32. Mitchison, T. J. (1989) *J. Cell Biol.* **109,** 637–652
33. Sawin, K. E. & Mitchison, T. J. (1991) *J. Cell Biol.* **112,** 941–954
34. Marklund, U., Larsson, N., Gradin, H. M., Brattsand, G. & Gullberg, M. (1996) *EMBO J.* **15,** 5290–5298
35. Howell, B., Deacon, H. & Cassimeris, L. (1999) *J. Cell Sci.* **112,** 3713–3722
36. Holmfeldt, P., Larsson, N., Segerman, B., Howell, B., Morabito, J., Cassimeris, L. & Gullberg, M. (2001) *Mol. Biol. Cell* **12,** 73–83
37. Kuntziger, T., Gavet, O., Sobel, A. & Bornens, M. (2001) *J. Biol. Chem.* **276,** 22979–22984
38. Curmi, P.A., Andersen, S. S., Lachkar, S., Gavet, O., Karsenti, E., Knossow, M. & Sobel, A. (1997) *J. Biol. Chem.* **272,** 25029–25036
39. Curmi, P. A., Maucuer, A., Asselin, S., Lecourtois, M., Chaffotte, A., Schmitter, J. M. & Sobel, A. (1994) *Biochem. J.* **300,** 331–338
40. Gamblin, T. C. & Williams, R. C., Jr. (1995) *Anal. Biochem.* **232,** 43–46
41. Panda, D., Samuel, S., Massie, M., Feinstein, S. C. & Wilson, L. (2003) *Proc. Natl. Acad. Sci. U. S. A.* **100,** 9548–9553
42. Bradford, M. M. (1976) *Anal. Biochem.* **72,** 248–254
43. Panda, D., Chakrabarti, G., Hudson, J., Pigg, K., Miller, H. P., Wilson, L. & Himes, R. H. (2000) *Biochemistry* **39,** 5075–5081
44. Srivastava, A. & Krishnamoorthy, G. (1997) *Anal. Biochem.* **249,** 140–146
45. Wong, P., Kleemann, H. W. & Tannock, I. F. (2002) *Br. J. Cancer* **87,** 238–245
46. Muller-Borer, J., Yang, H., Marzouk, S. A. M., Lemasters, J. J. & Cascio, W. E. (1998) *Am. J. Physiol.* **275,** H1937–H1947
47. Malinowska, I., Stelmaszczyk-Emmel, A., Wąsik, M. & Rokicka-Milewska, R. (2002) *Med. Sci. Monit.* **8,** 441–447
48. Leem, C. H., Lagadic-Gossmann, D. & Vaughan-Jones, R. D. (1999) *J. Physiol.* (*Lond.*) **517,** 159–180
49. Chaillet, J. R., Amsler, K. & Boron, W. F. (1986) *Proc. Natl. Acad. Sci. U. S. A.* **83,** 522–526
50. Trzaskawka, E., Vigo, J., Egea, J.-C., Goldsmith, M.-C., Salmon, J.-M. & De Periere, D. D. (2000) *Eur. J. Oral Sci.* **108,** 54–58
51. Gerboth, G. D., Effros, R. M., Roman, R. J. & Jacobs, E. R. (1993) *Am. J. Physiol.* **264,** L448–L457
52. Buckler, K. J. & Vaughan-Jones, R. D. (1990) *Pfluegers Arch. Eur. J. Physiol.* **417,** 234–239
53. Seksek, X., Henry-Toulmé, Sureau, F. & Bolard J. (1991) *Anal. Biochem.* **193,** 49–54
54. Stewart, A. K., Boyd, C. A. R. & Vaughan-Jones, R. D. (1999) *J. Physiol.* (*Lond.*) **516,** 209–217
55. Larsson, N., Segerman, B., Howell, B., Fridell, K., Cassimeris, L. & Gullberg, M. (1999) *J. Cell Biol.* **146,** 1289–1302
56. Steinmetz, M. O., Kammerer, R. A., Johnke, W., Goldie, K. N., Lustig, A. & van

Oostrum, J. (2000) *EMBO J.* **19,** 572–580
57. Ravelli, R. B., Gigant, B., Curmi, P. A., Jourdain, I., Lachkar, S., Sobel, A. & Knossow, M. (2004) *Nature* **428,** 198–202
58. Toso, R. J., Jordan, M. A., Farrell, K. W., Matsumoto, B. & Wilson, L. (1993) *Biochemistry* **32,** 1285–1293
59. Farrell, K. W., Jordan, M. A., Miller, H. P. & Wilson, L. (1987) *J. Cell Biol.* **104,** 1035–1046
60. Gradin, H. M., Larsson, N., Marklund, U. & Gullberg, M. (1998) *J. Cell Biol.* **140,** 131–141
61. Gavet, O., Ozon, S., Manceau, V., Lawler, S., Curmi, P. & Sobel, A. (1998) *J. Cell Sci.* **111,** 3333–3346
62. Arnal, I., Karsenti, E. & Hyman, A. A. (2000) *J. Cell Biol.* **149,** 767–774
63. Wilson, L., Panda, D. & Jordan, M. A. (1999) *Cell Struct. Funct.* **24,** 329–335
64. Gigant, B., Curmi, P. A., Martin-Barbey, C., Charbaut, E., Lachkar, S., Lebeau, L., Siavoshian, S., Sobel, A. & Knossow, M. (2000) *Cell* **102,** 809–816
65. Derry, W. B., Wilson, L. & Jordan, M. A. (1998) *Cancer Res.* **58,** 1177–1184
66. Grego, S., Cantillana, V. & Salmon, E. D. (2001) *Biophys. J.* **81,** 66–78
67. Tanaka, E. & Kirschner, M. W. (1995) *J. Cell Biol.* **128,** 139–155
68. Desai, A., Verma, S., Mitchison, T. J. & Walczak, E. (1999) *Cell* **96,** 69–78
69. Rogers, G. C., Rogers, S. L. & Sharp, D. J. (2005) *J. Cell Sci.* **118,** 1105–1116
70. Vorobjev, I. A., Svitkina, T. M. & Borisy, G. G. (1997) *J. Cell Sci.* **110,** 2635–2645
71. Vorobjev, I. A., Rodionov, V. I., Maly, I. V. & Borisy, G. G. (1999) *J. Cell Sci.* **112,** 2277–2289
72. Mcbeath, E. & Fujiwara, K. (1990) *Eur. J. Cell Biol.* **52,** 1–16
73. Waterman-Storer, C. M. & Salmon, E. D. (1997) *J. Cell Biol.* **139,** 417–434
74. Tanaka, E. M. & Kirschner, M. W. (1991) *J. Cell Biol.* **115,** 345–363